

# Research on High-precision Geometric Positioning of ZY-3

Qingxing YUE<sup>a</sup>, Xinming TANG<sup>a</sup>, Xiaoming GAO<sup>a</sup>

<sup>a</sup> Satellite Surveying and Mapping Application Center, NASG, Beijing, 101300, China (yueqx@sasmac.cn)

**ABSTRACT:** This paper established strict image-object relationship model of ZY-3, and analyzed orbital data and attitude data statistically. It did camera geometric calibration using high-precision artificial target. Internal geometric correction of the original satellite images, eliminating the interior orientation parameters such as non-uniform transition, transition of the integration time and attitude of high frequency components, achieved a high geometric positioning accuracy.

**Key words:** ZY-3, orbit, attitude, geometric calibration, geometric model

## 1. INTRODUCTION

ZY-3, the first civilian satellite of China with a stereo mapping function was successfully launched in January 2012. ZY-3 has mainly two functions, surveying & mapping and resources survey, and is used for production and update of 1:50000 stereo mapping and basic geographic information products, to carry out the investigation and monitoring of land and resources. ZY-3 equipped with four cameras, the backward camera, the nadir camera and the forward camera constitute three-line-array stereo surveying and mapping camera. The resolution of backward and forward camera is about 3.6 meters, and the resolution of nadir camera is about 2.1 meters, the resolution of multi-spectral camera is about 6 meters. The most important in high resolution stereo surveying and mapping is the geographic precision, and the decisive factor of geographic precision of stereo surveying and mapping is the geographic precision of imaging geographic model. The imaging geographic model of ZY-3 is composed by orbit parameter, attitude parameter, camera setting parameter and the inner orientation parameter. Firstly, this paper established the strict imaging geographic model. Then, it analyzed the relative precision of orbit data, and made statistical analysis on the frequency range of roll angel and pitch angel which affect the geographic precision obviously. It devised an interior and exterior parameter integration adjustment plan and makes an interior parameter adjustment and attitude system error adjustment using artificial target, and verified the adjustment precision with obvious features control points. Lastly, it makes interior geographic correction for L0 image using interior orientation parameters and high frequency attitude parameters, and makes comparative analysis of single image geographic precision and stereo intersection precision before and after correction. The result

indicates that the precision of single image and stereo intersection are both improved after correction.

## 2. ZY-3 STRICT GEOMETRIC MODEL

The strict geographic model of ZY-3 is the image-object relationship model using orbit parameter, attitude parameter, camera geographic setting parameter and camera interior orientation parameter.

The orbit parameter of ZY-3 is the satellite position and velocity vector  $(X_s, Y_s, Z_s, V_{xs}, V_{ys}, V_{zs})$  in WGS84 earth-correct coordinate system and the frequency is 1Hz. The rotation matrix array from local orbit coordinate system to WGS84 geocentric space Cartesian coordinate system  $r_{obt84toeth84}$  is acquired from the normalized satellite position and velocity vectors and their cross product. The attitude data is attitude quaternion between satellite body coordinate system and J2000 orthogonal coordinate system, which is the vector parameters  $(q_1, q_2, q_3)$ , and the scalar variable is:

$$q_0 = \sqrt{1 - (q_1^2 + q_2^2 + q_3^2)} \quad (1)$$

The rotation matrix array from satellite body coordinate system to J2000 geocentric space Cartesian coordinate system  $r_{plmtoeth2000}$  can be obtained from the attitude quaternion. The rotation matrix array from J2000 geocentric space Cartesian coordinate system to WGS84 geocentric space Cartesian coordinate system  $r_{eth2000toeth84}$  is decided by precession, pole motion, notation and Earth rotation parameters. The rotation matrix array between the camera measurement coordinate system and satellite body coordinate system is  $r_{set}$ . The setting position between camera optical nodes and satellite body coordinate system is  $(X_{set}, Y_{set}, Z_{set})$ , and is obtained

from laboratory parameters. Generally speaking, there will be system error in  $r_{plmtoeth2000}$  and  $r_{set}$ . But discriminate the two kinds of errors will be difficult and not necessary in application. It is supposed that rotation matrix array decided by the total error is  $r_{err}$ . The focal length is  $f$ , the main point is  $c_0$ , and the size of CCD is  $pix$ . The column coordinate of a CCD is  $c$ , the corresponding distortion in TDI directory is  $dx_c$  and the distortion cross TDI directory is  $dy_c$ . The pixel vector  $u$  in camera measurement coordinate system is:

$$u = \begin{bmatrix} u_0 \\ u_1 \\ u_2 \end{bmatrix} = \begin{bmatrix} dx_c * pix \\ (c - c_0 + dy_c) * pix \\ -f \end{bmatrix} \quad (2)$$

This vector in WGS84 orthogonal coordinate system is  $u' = [u'_0, u'_1, u'_2]^T$ :

$$u' = r_{eth2000toeth84} * r_{plmtoeth2000} * r_{err} * r_{set} * u \quad (3)$$

The setting vector of camera optical nodes in WGS84 geocentric space Cartesian coordinate system is:

$$\begin{bmatrix} X'_{set} \\ Y'_{set} \\ Z'_{set} \end{bmatrix} = r_{eth2000toeth84} * r_{plmtoeth2000} * r_{err} \begin{bmatrix} X_{set} \\ Y_{set} \\ Z_{set} \end{bmatrix} \quad (4)$$

The position of camera optical nodes in WGS84 geocentric space Cartesian coordinate system is:

$$\begin{bmatrix} X_{opt} \\ Y_{opt} \\ Z_{opt} \end{bmatrix} = \begin{bmatrix} X_{opt} \\ Y_{opt} \\ Z_{opt} \end{bmatrix} + \begin{bmatrix} X'_{set} \\ Y'_{set} \\ Z'_{set} \end{bmatrix} \quad (5)$$

Suppose the corresponding ground point is  $M(X, Y, Z)$ , and the vector  $U$  from  $M$  to camera optical nodes is:

$$U = \begin{bmatrix} U_0 \\ U_1 \\ U_2 \end{bmatrix} = \begin{bmatrix} X_{opt} - X \\ Y_{opt} - Y \\ Z_{opt} - Z \end{bmatrix} \quad (6)$$

The final imaging geographic model is:

$$\frac{u'_0}{U_0} = \frac{u'_1}{U_1} = \frac{u'_2}{U_2} \quad (7)$$

### 3. ZY-3 ORBIT DATA ANALYSIS

The original GPS data of ZY-3 include the position and velocity vector and all original observation data of one GPS, and these data is the rough orbit data. The accurate orbit data can be obtained from all GPS data.

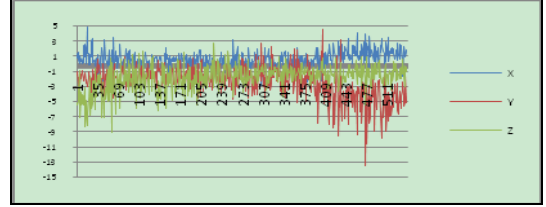


Figure 1. error of rough orbit compared with precision orbit

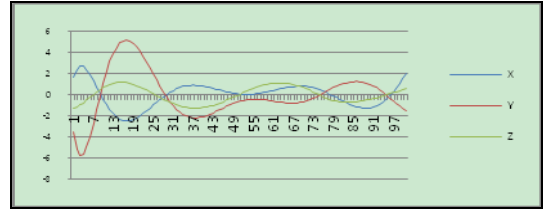


Figure 2. error of rough orbit by second-order polynomial fitting

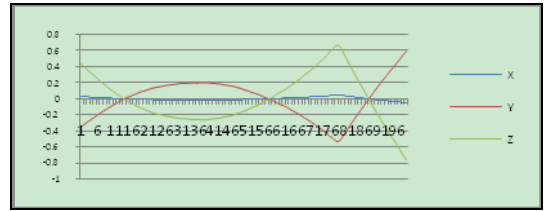


Figure 3. error of precision orbit by second-order polynomial fitting

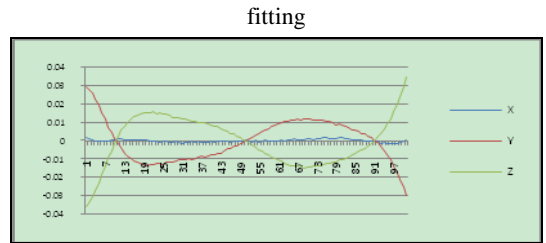


Figure 4. error of precision orbit by second-order fitting and a fixed integration time

Figure 1 shows the position statistical result of one GPS of ZY-3, it can be seen that the error is random and the wage is below 10 meters. Figure 2 shows the second order approximate error of the rough GPS data in the image of a scene (the interpolation data by Lagrange polynomial). It can be seen that the maximum error in Y direction is nearly 6 meters. Figure 3 shows the second-order polynomial fitting error of the accurate GPS data in one image scene, the turning part of the line is caused by the inhomogeneous of integration time. Figure 4 shows the second-order polynomial fitting error of the accurate GPS data in the image of a scene when the integration time is the same, the fitting error is below 5 centimeters.

#### 4. ZY-3 ATTITUDE DATA ANALYSIS

On the no-side-view imaging condition, the control and adjust of ZY-3 attitude is based on the nadir camera. It demands the front view camera imaging in the upright direction. The “upright” here means the angles between satellite body coordinate system and J2000 local orbital coordinate system include roll angle and pitch angle are 0, and the yaw angle equals to the theoretical drift angle. It can also be considered that the angles between satellite body coordinate system and WGS84 local orbital coordinate system include roll angle, pitch angle and yaw angle are all 0. This paper adopts the later definition. Suppose the rotation matrix from satellite body coordinate system to WGS84 local orbital coordinate system is  $r_{plmtoobr84}$ , there is:

$$r_{obt84toeth84} * r_{plmtoobr84} = r_{eth2000toeth84} * r_{plmtoeth2000} \quad (8)$$

And then:

$$r_{plmtoobr84} = r_{obt84toeth84}^{-1} * r_{eth2000toeth84} * r_{plmtoeth2000} \quad (9)$$

Lastly, compute the pitch, roll and yaw angle from  $r_{plmtoobr84}$  according to the  $(Y, X, Z)$  rotation system.

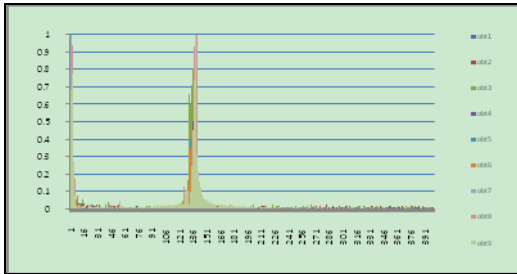


Figure 5. Spectrum statistical results of roll angle

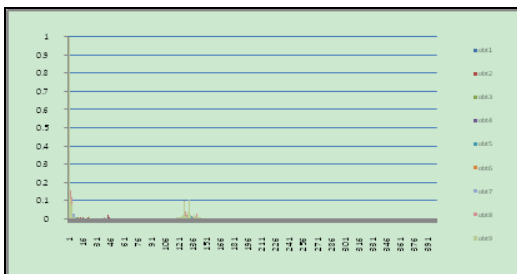


Figure 6. Spectrum statistical results of pitch angle

Figure 5 and Figure 6 are the normalized frequency spectrum statistical results of roll and pitch angle of 9 orbits, and the attitude frequency is 4Hz. The high frequency part of roll angle

is concentrated in the 1.35Hz, and the high frequency part of pitch angle is concentrated in 1.30Hz.

#### 5. THE INTERIOR CAMERA CALIBRATION BASED ON ARTIFICIAL TARGET

For the sake of high resolution geographic calibration of ZY-3, we laid down high precision artificial target, and measured a lot of obvious features control points. The backward, forward, nadir and multi-spectral image was obtained in February 2012. Figure 7 shows the distribution of the targets, and Figure 8 shows the ZY-3 images of the targets, the 31 targets form two horizontal rows and two vertical ranks. The distance between two horizontal rows is about 1300 meters. The interior camera adjustment uses the two horizontal rows to reduce the effect of instability of exterior orientation parameters. Figure 9 shows the variation of pitch, roll and yaw angle between satellites body coordinate system and WGS84 local orbital coordinate system are nearly linear. The variation is shown in chart 1. The variation of pitch is 0.000042 degree, which is equivalent to a distance about 0.37 meters, the variation of roll is 0.00013 degree, which is equivalent to a distance about 1.16 meters, the variation of yaw is 0.00008 degree, which is equivalent to 0.02 pixel of nadir camera.

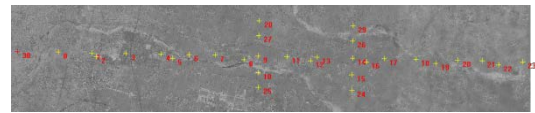


Figure 7. distribution diagram of artificial targets

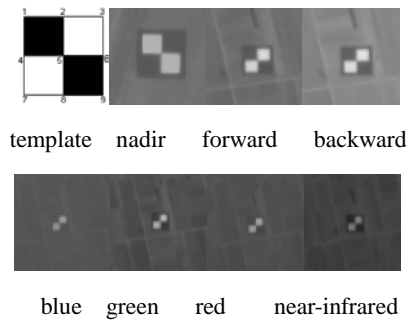


Figure 8. artificial targets imaging results of three-line-array cameras and multi-spectral camera of zy3

The image point of artificial target is obtained from least square match between gauss filtered template and target image. As shown in Figure 8, there are 9 feature points in every target image; the ground point coordinate of the feature point is measured by GPS. The precision of 5<sup>th</sup> point is the best, and it

will be used as control point. The other 8 points are measured in nadir image. The matched points between nadir image and other image are used as tie points.

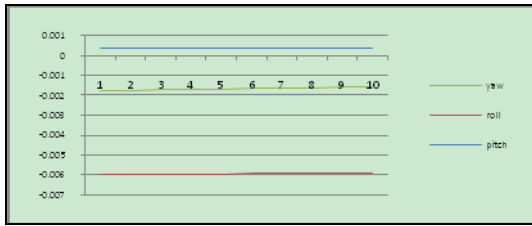


Figure 9. the three-axis attitude in corresponding period of artificial targets

Attitude(degree)	Pitch	roll	yaw
max	0.000395	-0.006395	0.004258
min	0.000353	-0.006263	0.004339
variable	0.000042	-0.00013	-0.00008

Table 1. the statistic result of three attitudes in imaging time of targets

The flow of adjustment is as follows:

- (1) Set a smaller focal length  $f$ , calculate the pixel vector  $u$  according to ideal linear CCD array:

$$u = \begin{bmatrix} u_0 \\ u_1 \\ u_2 \end{bmatrix} = \begin{bmatrix} 0 \\ (c - c_0) * pix \\ -f \end{bmatrix} \quad (10)$$

- (2) Establish the error equation according to equation (7), and calculate pitch, roll and yaw by least square method. The slewing rate is calculated from data of Chart 1. The three angles are variables of  $r_{err}$ .

- (3) Calculate the system error of the three angles and statistic the mean square error of control points.
- (4) Increase  $f$  according to a step (for example 0.01mm), calculate the system error of the three angles and statistic the mean square error of control points. Find the  $f$  corresponding to the least mean square error, the system error is the ideal exterior orientation parameter.
- (5) Calculate the image point ( $r'$ ,  $c'$ ) of ground control point according to pitch, roll, yaw and  $f$  through equation (7). The measured coordinate is ( $r$ ,  $c$ ), and the distortion of column  $c$  is:

$$dx_c = r - r', \quad dy_c = c - c'$$

- (6) Add the distortion of the 5<sup>th</sup> point to all the other 8

corresponding tie points; calculate the ground points by forward intersection. These points are used as ground control points of tie points. Here they are called "tie control point".

- (7) Repeat (1)-(6) using "tie control point" and measured control points as control data. Calculate the variation of distorting of twice results, stop repeating if the maximum variation is smaller than a threshold.
- (8) Calculate the distortion of every CCD column using distortion of control points through a second-order polynomial and every CCD array will be calculated separately.

The final distortion includes the optical distortion and CCD distortion.

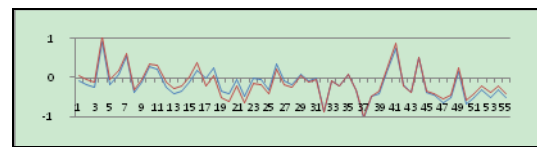
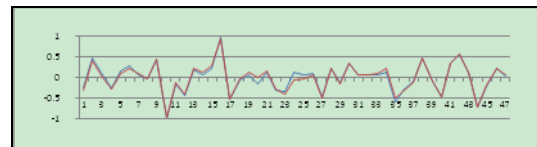


Figure 10. error comparison of backward image before(blue) and after(red) calibration (as-up, cs-down)

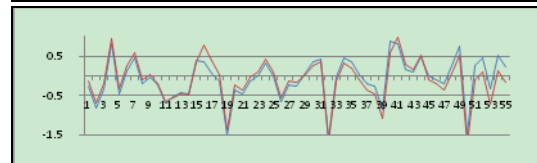
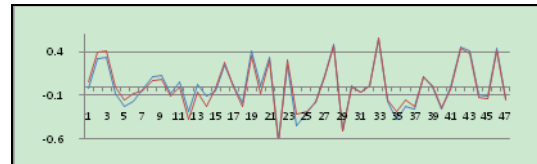


Figure 11. error comparison of forward image before(blue) and after(red) calibration (as-up, cs-down)

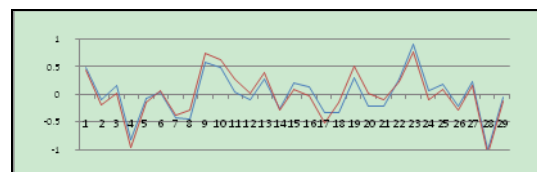
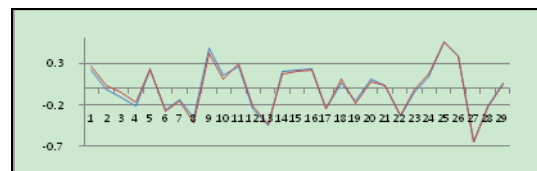


Figure 12. error comparison of downward image before(blue) and after(red) calibration (as-up, cs-down)



Figure 13. error comparison of blue-band image before(blue) and after(red) calibration (as-up, cs-down)

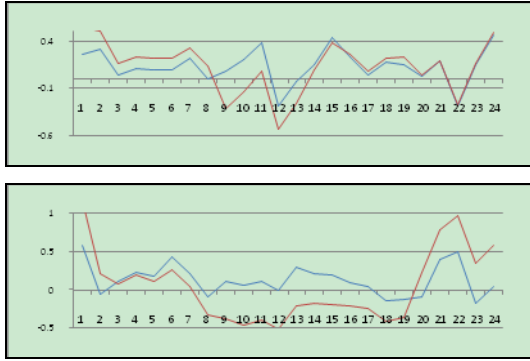


Figure 14. error comparison of green-band image before(blue) and after(red) calibration (as-up, cs-down)

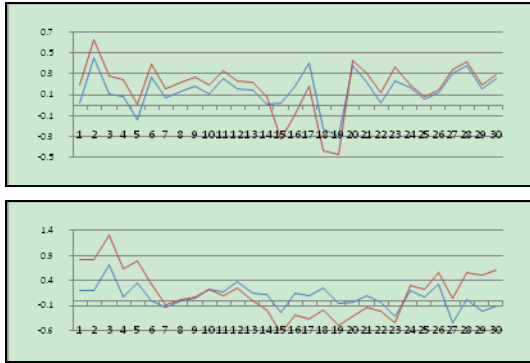


Figure 15. error comparison of red-band image before(blue) and after(red) calibration (as-up, cs-down)

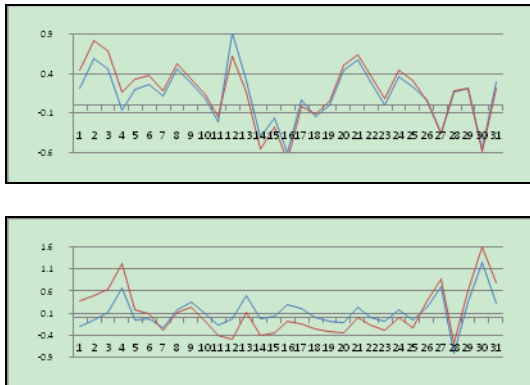


Figure 16. error comparison of near-infrared-band image

before(blue) and after(red) calibration (as-up, cs-down)

## 6. ZY-3 INTERIOR GEOGRAPHIC CORRECTION AND GEOGRAPHIC POSITIONING PRECISION

The strict geographic model has too many parameters, every image column has two distortion parameters and every image row has a group of exterior orientation parameters. So the application is sophisticated and not convenient in the later data process. This paper reimaging the original image (called corrected image) by re-sampling on the condition that the CCD array is linear (no distortion) and the attitude has no high frequency part. The flow of correction is as follows:

- (1) The three attitude array between satellite body coordinate system and WGS84 local orbital coordinate are:

$$\begin{aligned} &pitch_0, pitch_1, \dots, pitch_n \\ &roll_0, roll_1, \dots, roll_n \\ &yaw_0, yaw_1, \dots, yaw_n \end{aligned}$$

Approximate the attitude curve by a linear fit.

- (2) Every attitude in the attitude array subtract the line approximated attitude, the difference array is the high frequency attitude array:

$$\begin{aligned} &pitch'_0, pitch'_1, \dots, pitch'_n \\ &roll'_0, roll'_1, \dots, roll'_n \\ &yaw'_0, yaw'_1, \dots, yaw'_n \end{aligned}$$

Suppose there is a point in the corrected image, the row is  $i$  and the column is  $j$ . The corresponding point in original point ( $r, c$ ) is:

$$\begin{aligned} r &= i + dx_j + pitch'_i * f / pix + yaw'_i * (j - c_0) \\ c &= j + dy_j + roll'_i * f / pix \end{aligned}$$

(12)

- (3) Calculate every image point in original image of every corrected image point, get the DN of corrected image by bilinear interpolation.

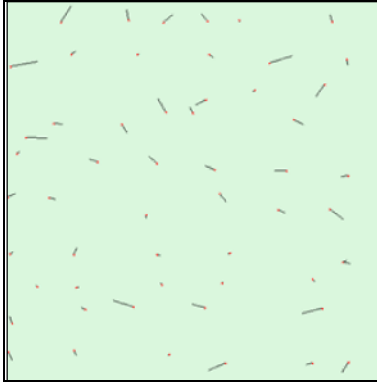


Figure 17. error distribution of backward image before calibration

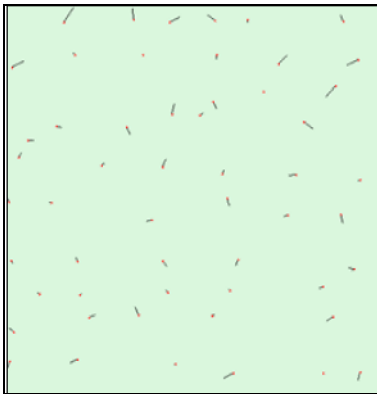


Figure 18. error distribution of backward image after calibration

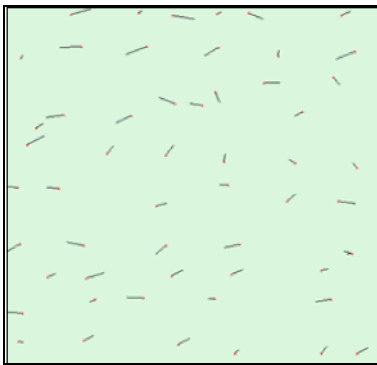


Figure 19. error distribution of forward image before calibration

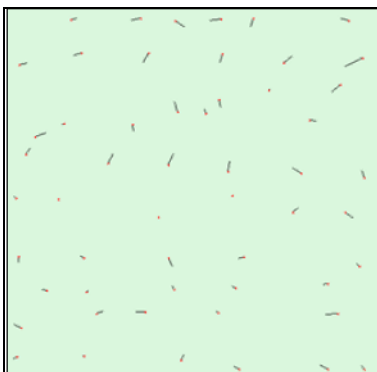


Figure 20. error distribution of forward image after calibration

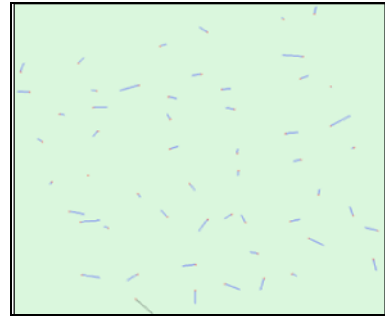


Figure 21. plane accuracy of object side before calibration (RMS\_x:1.91m, RMS\_y:1.29m)

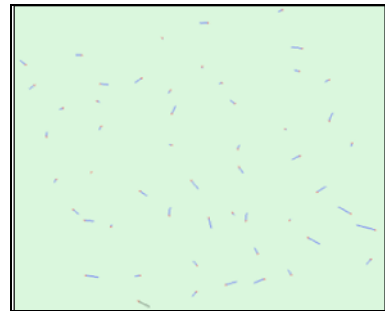


Figure 22. plane accuracy of object side after calibration (RMS\_x:1.31m, RMS\_y:0.98m)

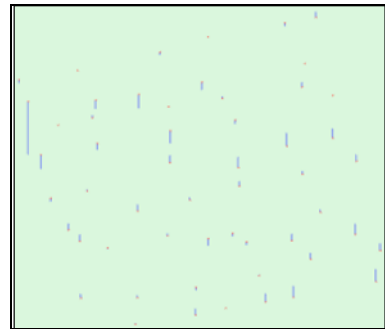


Figure 23. elevation accuracy of object side before calibration (RMS\_h:1.82m)

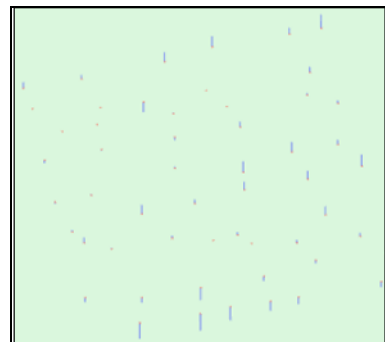


Figure 24. elevation accuracy of object side after calibration (RMS\_h:1.47m)

## 7. CONCLUSION

The relative error between rough GPS data and precision GPS data is below 10 meters, and the rough GPS data curve is not

smooth. There are steps in integration time, which causes a fitting error about 0.7 meters. The high frequency part of attitude is stable, and the amplitude of roll angle is larger. Corrected the interior geographic distortion by high precision artificial target, and check the improvement of correction using obvious features control points. For the three-line-array cameras are surveying and mapping cameras. The interior distortion caused by CCD and optical distortion is not obvious. So it does not affect the geographic positioning accuracy

obviously. The multiband camera is not surveying and mapping camera and the improvement is obvious. The high frequency part of attitude will affect the geographic precision obviously. The traditional polynomial fitting will cause a larger error. After correction of original image using the calibrated interior parameters and high frequency part of attitude data, the plane precision and elevation precision are all improved obviously. But there is still some system error because of the attitude error, and it is suggested to improve by block adjustment.

## REFERENCES

- Mathias Schneid. STEREO EVALUATION OF ALOS/PRISM DATA ON ESA-AO TEST SITES - FIRST DLR RESULTS, ISPRS 2008, Vol. XXXVII. Part B1, pp.739-744.
- K. Jacobsen. SATELLITE IMAGE ORIENTATION, ISPRS 2008, Vol. XXXVII. Part B1, pp.703-710.
- T. Weser. AN IMPROVED PUSHBROOM SCANNER MODEL FOR PRECISE GEOREFERENCING OF ALOS PRISM IMAGERY, ISPRS 2008, Vol. XXXVII. Part B1, pp.723-730.
- F. de Lussy. PROCESS LINE FOR GEOMETRICAL IMAGE CORRECTION OF DISRUPTIVE, ISPRS 2008, Vol. XXXVII. Part B1, pp.27-34.
- T.Tadono. CALIBRATION AND VALIDATION OF PRISM ONBOARD ALOS. ISPRS 2008, Vol. XXXVII. Part B1.
- S. Bauer. EVALUATION OF CAMERA CALIBRATION APPROACHES FOR VIDEO IMAGE DETECTION SYSTEMS, ISPRS 2008, Vol. XXXVII. Part B1.
- Junichi Takaku. PRISM On-Orbit Geometric Calibration and DSM Performance, IEEE TRANSACTIONS ON GEOSCIENCE AND REMOTE SENSING, 47(12), DECEMBER 2009, pp.4060-4073.
- Junichi Takaku. RPC GENERATIONS ON ALOS PRISM AND AVNIR-2, 2011 IEEE, pp.539-542.
- Wang zhizhuo, PHOTOGRAMMETRIC PRINCIPLE. 1979.
- Wang Renxiang. SATELLITE PHOTOGRAMMETRIC PRINCIPLE FOR THREE-LINE-ARRAY CCD IMAGERY. 2006.